DSC and X-ray Studies of a Thermotropic Four-Monomer Copolyester

Rolf Löffler and Patrick Navard*

Ecole Nationale Supérieure des Mines de Paris, Centre de Mise en Forme des Matériaux, URA CNRS 1374, BP 207, 06904 Sophia Antipolis Cedex, France

Received February 27, 1992; Revised Manuscript Received September 3, 1992

ABSTRACT: The thermotropic main chain copolyester consisting of terephthalic acid (TA), methylhydroquinone (MHQ), 4-hydroxybenzoic acid (HBA) and 4,4'-dicarboxydiphenyl ether (DDE), has at room temperature an orthorhombic unit cell which contains two polymer chains. Annealing or quenching of the product does not change its structure. The lattice constants are a = 9.52 Å and b = 5.31 Å and the c-axis which lies in the direction of the chains has an average value of c = 13.4 Å. Nonisothermal crystallization showed several melting peaks depending on the cooling rate, indicating that crystals with different sizes and levels of perfection exist. The highest melting temperature for nonisothermally crystallized samples was always 297 °C, and the crystals are metastable. The melting temperature could be increased by annealing at elevated temperatures up to 320 °C, and the heat of fusion ΔH could be raised from about 1.4 up to 2.8 kJ/mol. The equilibrium thermodynamic properties of the copolymer were found to be $T_m°$ = 355 °C, $\Delta H°$ = 6 kJ/mol, and $\Delta S°$ = 9.6 J/(mol K). There exist two crystallization processes, a fast one and a slow one. The fast process has an Avrami exponent of n = 2, indicating a two-dimensional growth, which is in agreement with a thermally induced nucleation and growth mechanism for rigid rodlike molecules. The kinetics of the slow crystallization process (secondary crystallization) show that the degree of crystallinity increases linearly with the logarithm of time. The activation energy of the slow process follows an Arrhenius behavior and has a value of 1.86 kJ/mol, indicating that the slow crystallization process is not cooperative.

Introduction

The crystallization behavior and the crystalline structure of thermotropic liquid crystalline polymers (LCP's) has been extensively studied during the last 10 years, because the ultimate mechanical properties of this class of materials strongly depend on the solid structure (crystallinity and morphology) and on the thermal and mechanical history of the polymer during processing.[1-5] Rigid rodlike homopolymers with a regular structure usually decompose before the solid to nematic phase transition is reached and cannot be processed. One possibility for lowering the melting point is to copolymerize different aromatic ester monomers to disturb the regularity of the crystalline structure along the chain axis. Another possibility is to introduce a kink or bulky side group which disturbs the regularity of the lateral packing. These irregularities result in an increase of the transition entropy and a decrease of the transition enthalpy, thus causing a decrease of the melting point.

To a large extent the complex structure of the solid state results from the thermal history in the nematic state and from supercooling during the phase transition,[6] in addition to the chemical change. It has also been reported that the melting temperatures of LCP's are significantly raised by annealing in the solid state[1] or in the molten state above the nominal melting temperature.[5]

Kinetic studies of the phase transitions have shown for different LCP's that two transition processes exist:[1-3,7,8] a fast process which has a high melting transition temperature while its enthalpy of fusion is only very slightly influenced by annealing time; a slow transition process which can be observed by the development of a second transition peak at lower temperatures, which shifts to higher temperatures and shows an increase of the melting enthalpy during annealing. Additionally, the formation of other crystalline structures has been reported during annealing.[3,8]

Most of the reported studies have been performed with a commercial two-monomer copolyester with different compositions of *p*-hydroxybenzoic acid (HBA) and 6-hydroxy-2-naphthoic acid (HNA).[1,2,7-12] Wide-angle X-ray diffraction analysis on HBA/HNA copolymers over the entire composition range has shown that the crystals of the copolyesters are aperiodic in the direction of the chain axis and show some three-dimensional order. Two models have been proposed to describe the solid-state structure of these LCP's. Windle and co-workers have suggested that short identical sequences in random copolymer chains like HNA/HBA match each other laterally, forming nonperiodic layer crystals (NPL) that have a three-dimensional order.[9] Blackwell and co-workers have proposed another model which suggests that the development of the three-dimensional order only requires that one monomer unit on each chain lie about a register plane perpendicular to the chain axis; the lateral matching of identical copolymer sequences is not regarded as a necessary condition to form aperiodic crystals.[10] It had also been reported that solid-state annealing of LCP's increases the crystallite size, as indicated by sharpened wide-angle X-ray diffractions and increased DSC melting temperatures.[1,11] Additionally, the phase-transition behavior of LCP's may be further complicated by transesterifications in the nematic state, forming insoluble and infusible block copolymers.[8]

Several questions have arisen about the general meaning of the two crystallization processes and the structural interpretation of the X-ray scattering. One way to answer these questions is to use a large variety of different thermotropic polymers. Our contribution will consist of studying a four-monomer random copolyester by DSC and X-ray scattering. Its thermal behavior and its crystalline structure will be compared to the above results.

Experimental Section

The synthesis of the investigated copolyester which is composed of four monomeric units (terephthalic acid (TA), methylhydroquinone (MHQ), 4-hydroxybenzoic acid (HBA) and 4,4'-dicarboxydiphenyl ether (DDE)) is described in detail in ref 13 and shows a nematic melt above its crystalline melting temperature.

The received polymer pellets were dried under vacuum at 120 °C for 8 h. Isotropic samples were obtained by compressing films

0024-9297/92/2225-7172$03.00/0

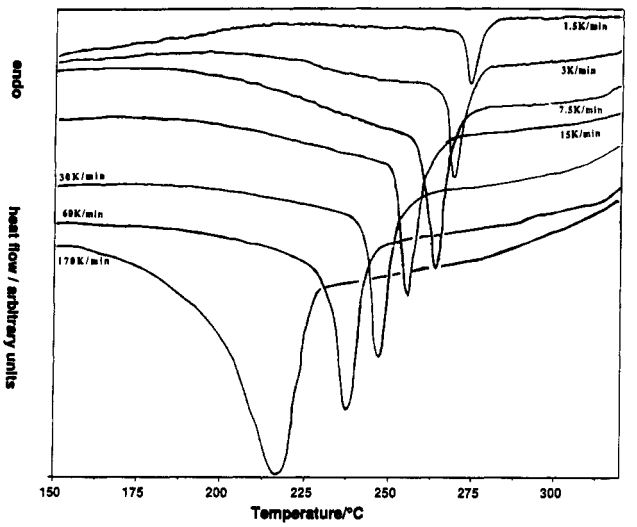

Figure 1. DSC cooling traces from the nematic melt at $T = 330$ °C for different cooling rates.

from the pellets at a temperature of 310 °C. Fibers were obtained by melt-drawing. The samples which showed an amorphous character when examined by wide-angle X-ray diffraction were prepared in the following manner. The polymer was first dissolved in a solution of 50% wt *p*-chlorophenol and 50% wt 1,2-dichlorethane and then precipitated into a solution of 70% vol 1,2-dichlorethane and 30% vol acetone. The precipitate was washed three times with this solution to remove the *p*-chlorophenol. Afterward the precipitate was dried under vacuum at 70 °C.

The thermal properties were investigated with a Perkin-Elmer DSC-7 calorimeter. Both temperature and heat flow were calibrated with indium and lead. Samples were punched out from the prepared film to fit exactly into the aluminum pans. The sample weights were in the range 19–21 mg. All thermal analyses were run under a dry nitrogen atmosphere.

To prevent self-nucleation[14] and to always start from the same standard conditions, the sample was heated before each experiment to 330 °C for 1 min before further manipulations.

For nonisothermal crystallization experiments, the samples were cooled down to 150 °C with different cooling rates (from 1.5 to 170 °C/min).

For isothermal crystallization experiments the samples were quenched (200 °C/min, with the intercooler on) from 330 °C to a predetermined crystallization temperature and kept there for different fixed periods of time. The samples were heated directly afterward at a rate of 15 °C/min above their transition temperature, and the heating traces were recorded.

The X-ray analysis was carried out with a Phillips wide-angle diffractometer and a flat film camera, using either a photographic film or a position-sensitive detector to record X-ray diffraction. Ni-filtered Cu Kα radiation with a wavelength of $\lambda = 1.542$ Å was used.

Results and Discussion

DSC Experiments. (I) Crystallization at Various Cooling Rates and Subsequent Heating. Figure 1 shows nonisothermal cooling traces of the copolymer from its nematic melt at different cooling rates, and Figure 2 shows the subsequent heating traces. An increase in cooling rate results in a shift of the location of exothermic peak to lower temperatures, as can be seen in Figure 1, while the location of the highest melting peak (297 °C) for the subsequent heating runs (Figure 2) is independent of the cooling rate.

An interesting finding is that, for cooling rates up to 15 °C/min in addition to a fast transition process (sharp peak), a slow process (secondary crystallization process) can be observed. The heat flow change of this slow process can be observed down to a temperature of 210 °C. At higher cooling rates, this slow process is not seen due to the occurrence of the fast transition process in the same

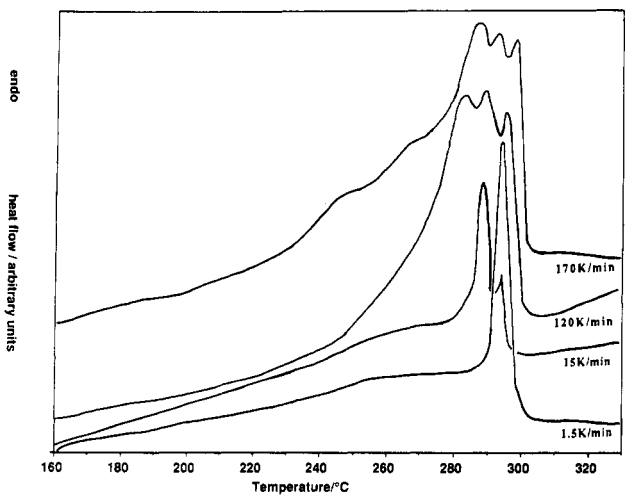

Figure 2. DSC heating traces (15 °C/min) of samples crystallized nonisothermally.

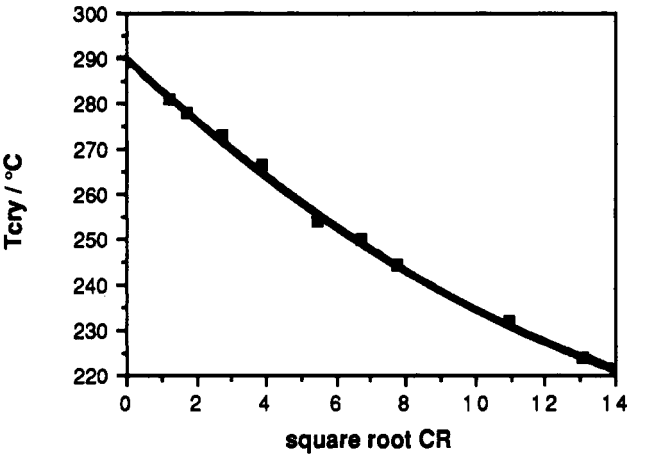

Figure 3. Square root of the cooling rate (°C/min) vs the beginning of crystallization.

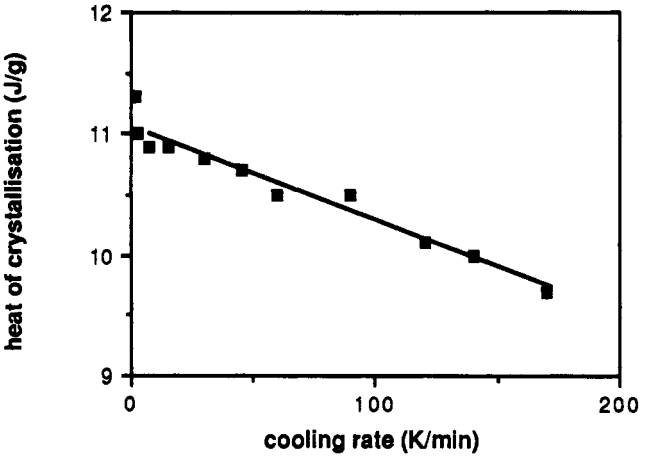

Figure 4. Dependence of the enthalpy of crystallization vs different cooling rates.

temperature range. Extrapolation to zero cooling rate of the temperature when crystallization starts is shown in Figure 3 and reveals that 290 °C is the temperature down to which the nematic melt can be cooled without the beginning of the crystal growth. This extrapolated value lies near the temperature of the highest melting peak of the metastable crystals. The polymer can be supercooled down to 60 °C under its metastable nematic melt by imposing a high cooling rate of 170 K/min and there is a slight decrease of the crystallization enthalpy with raising cooling rate (Figure 4). It is not possible to suppress the crystallization process by quenching the polymer on cold water.

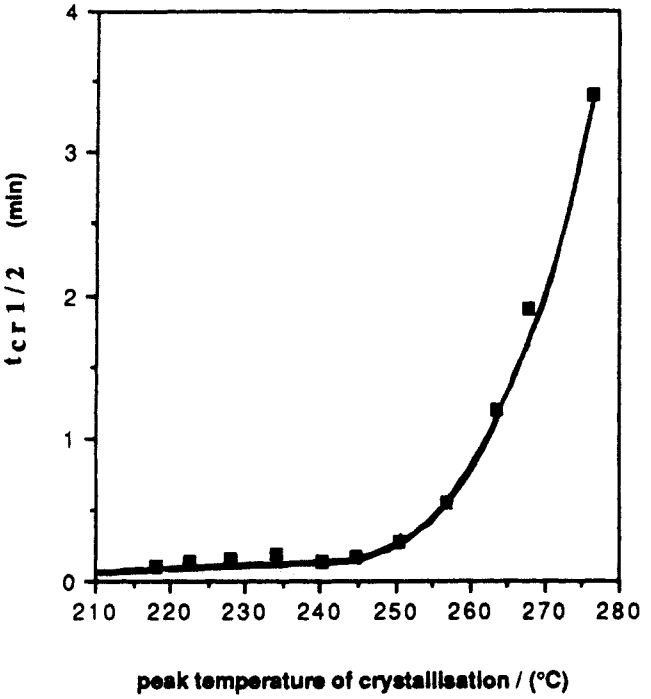

Figure 5. Relationship between the half-time of the fast crystallization process $t_{cr/2}$ and the maximum peak temperature of crystallization for different cooling rates.

The width of the sharp crystallization peak at half-height divided by the cooling rate yields the time $t_{cr/2}$ necessary for performing half of the fast transition process at a given crystallization temperature (maximum crystallization peak). Values of this time $t_{cr/2}$ range from 3.4 min at a cooling rate of 1.5 °C/min to 0.1 min at a cooling rate of 170 °C/min. In Figure 5 this time $t_{cr/2}$ is plotted against the maximum peak temperature of crystallization. One can clearly see that the more the nematic melt is supercooled, the faster the crystallization takes place. These observations indicate that the fast process can only be studied in a temperature range between 280 and 290 °C. At higher temperatures the nematic phase is metastable, while at temperatures below 280 °C the fast transition process is too quick.

The subsequent heating traces after nonisothermal crystallization (Figure 2) show an increase in the number of distinct melting peaks from two at a cooling rate of 1.5 °C/min to five at a cooling rate of 200 °C/min. These observations are in contrast to data reported for other LCP copolymers[1-3,7] which show only one peak of fusion.

(II) Isothermal Crystallization. The temperature range of the isothermal crystallization studies was between 220 and 287 °C. To elucidate the two different crystallization processes, we have split the isothermal crystallization studies in two parts. The first is concerned with the temperature range from 287 to 280 °C where it is possible to study the fast transition process. The second part is concerned with the slow transition process.

Isothermal Crystallization To Investigate the Fast Transition Process. When the isothermal experiments were carried out above 280 °C, only one endothermic melting peak was observed after different crystallization times (Figure 6). The melting temperature and the heat of fusion ΔH are shifted continuously with time to higher values. Changes of the heat of fusion with respect to the logarithm of the crystallization time are plotted in Figure 7 for three temperatures (280, 283, and 287 °C). The curves show two different regions. For short crystallization times t, an exponential behavior between the heat of fusion and log t is found (fast crystallization process), while at longer

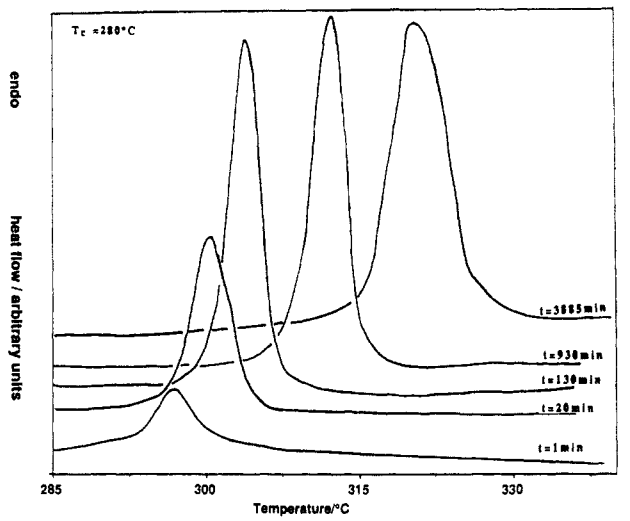

Figure 6. Set of DSC heating traces after isothermal crystallization at T_c = 280 °C for different times t.

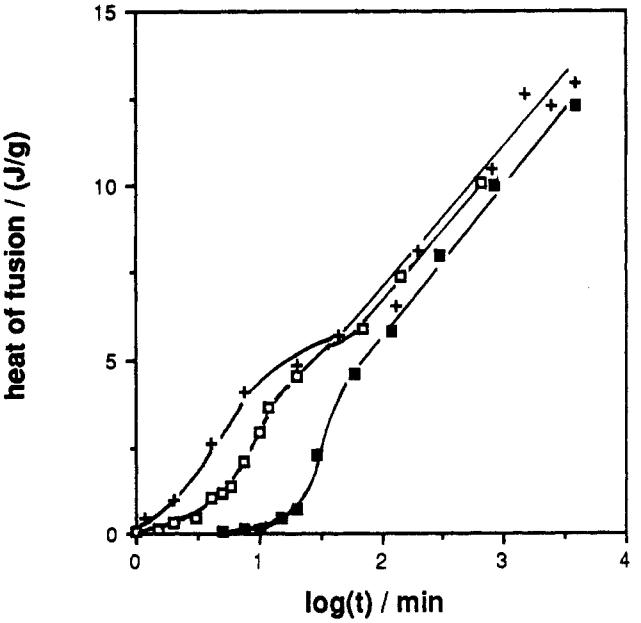

Figure 7. Relationship between the heat of fusion ΔH against the logarithm of crystallization time t for three different temperatures: T_c = 280 °C (+); T_c = 283 °C (□); T_c = 287 °C (■).

times the curves slow down to become linear (slow crystallization process). That means that (a) ΔH and t are proportional for the fast crystallization process and (b) a linear relation between ΔH and log t is found for the slow process.

Isothermal Crystallization To Investigate the Slow Transition Process. To investigate the slow transition process, we performed isothermal crystallization experiments for long periods of time. As an example Figure 8 shows a set of DSC melting traces after isothermal annealing (crystallization) at T_c = 250 °C for different lengths of time. For a short time period (1 min), four transition peaks can be identified, in contrast to the HBA/HNA copolymers where only one peak is found.[1,2,7] With increasing time, the lowest peak gets more pronounced and it is shifted to higher temperatures. After a crystallization time of 895 min, only one peak exists which is shifted further to a higher melting temperature with prolonged crystallization time. It is also found that the heat of fusion of this single peak increases with annealing time.

In Figure 9, the development of the melting temperatures of the two highest melting peaks with respect to log

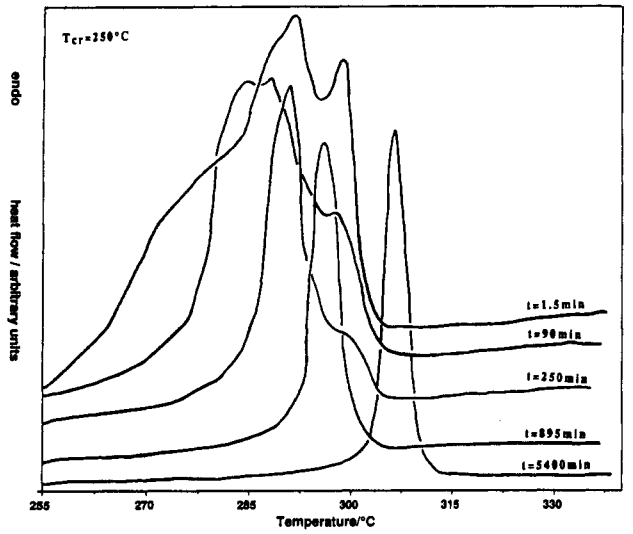

Figure 8. Set of DSC heating traces after isothermal crystallization at T_c = 250 °C for different times t.

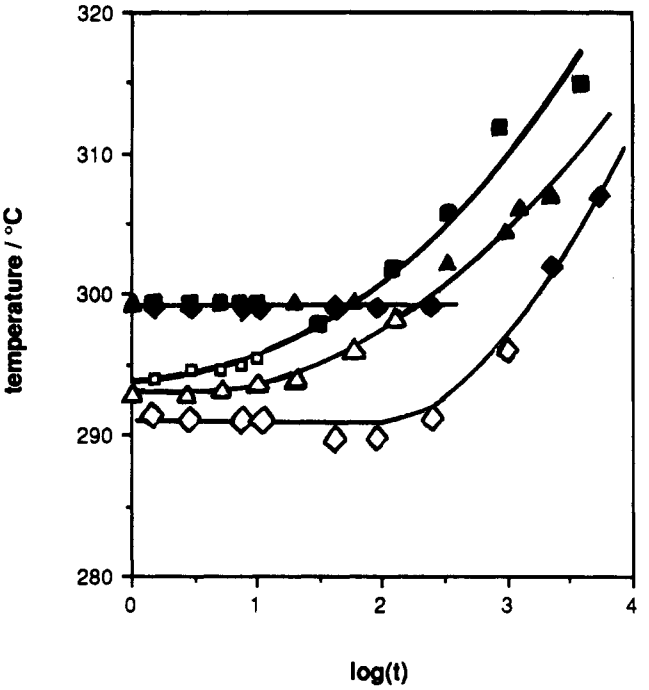

Figure 9. Relationship of the melting temperatures of the two highest melting peaks with respect to the logarithm of crystallization time for three different temperatures: T_c = 273 °C (□, ■); T_c = 265 °C (Δ, ▲); T_c = 250 °C (◇, ◆). The filled symbols represent the highest melting peak; the open symbols represent the second highest melting peak.

t for three crystallization temperatures is shown. First the highest melting peak is not influenced by annealing until the lower melting peak has reached it. Afterward, only the existing peak is shifted to higher temperatures. Shifting of the melting peaks becomes more effective when the temperature is raised.

In Figure 10 for several temperatures the overall heat of fusion is plotted against log t. One can see that ΔH is increased by lowering the crystallization temperature. At the two lowest crystallization temperatures there is a linear relationship between the heat of transition and logarithmic crystallization time. Such linear behavior has been reported for HBA/HNA polymers.[1,2] At higher crystallization temperatures, two different regions are found. The first region still shows a contribution of the fast process. At longer crystallization times (more then 10 min) the curve is linear, indicating that only one process (slow process) contributes to ΔH. The relationship between the heat of fusion ΔH and the logarithmic crystallization time

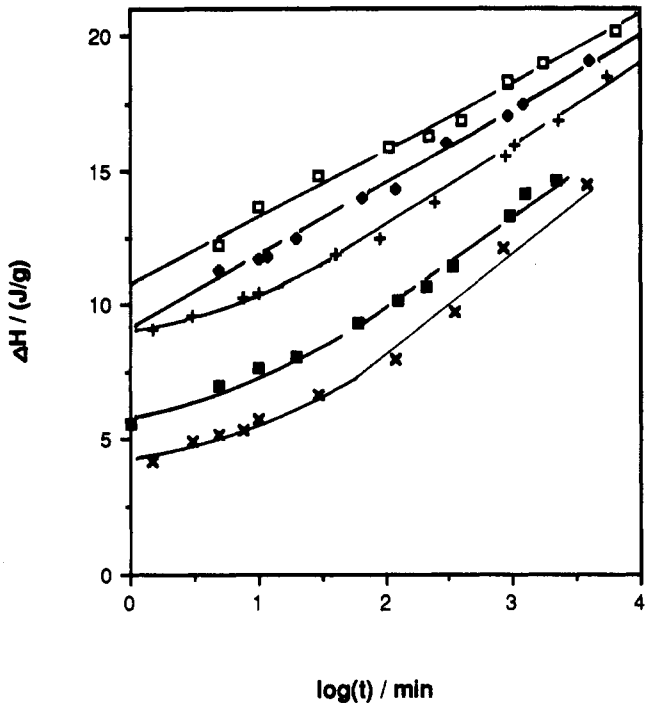

Figure 10. Relationship between the heat of fusion ΔH and the logarithm of crystallization time t for five different temperatures: T_c = 220 °C (□); T_c = 235 °C (♦); T_c = 250 °C (+); T_c = 265 °C (■); T_c = 273 °C (×).

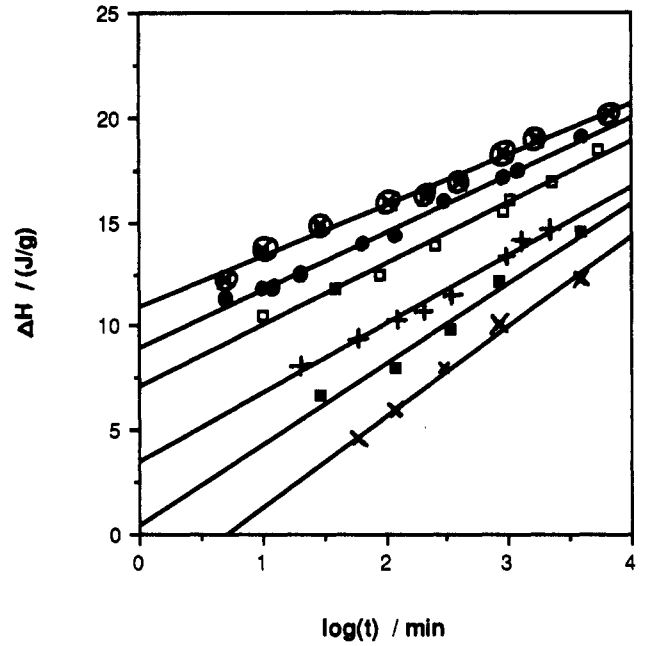

Figure 11. Extrapolation of the linear regimes of the heat of fusion against the logarithm of time t for six different temperatures to determine their velocity rate $A(T_c)$: T_c = 220 °C (⊛); T_c = 235 °C (●); T_c = 250 °C (□); T_c = 265 °C (+); T_c = 273 °C (■); T_c = 287 °C (×).

log t for different crystallization temperatures T_c can therefore be described as

$$\Delta H(T_c,t) = A(T_c) \log (t) + B(T_c,t) \quad (1)$$

$A(T_c)$ is a parameter which determines the velocity of the slow transition. $B(T_c,t)$ gives the contribution of the fast process and becomes constant when the fast process is completed.

In Figure 11 only the linear regimes are extrapolated to determine $A(T_c)$. As can be seen from the slopes, the slow process becomes faster the higher the crystallization temperature T_c is. An increase of $A(T_c)$ from 351 J/mol at T_c = 220 °C to 621.9 J/mol at T_c = 287 °C was measured.

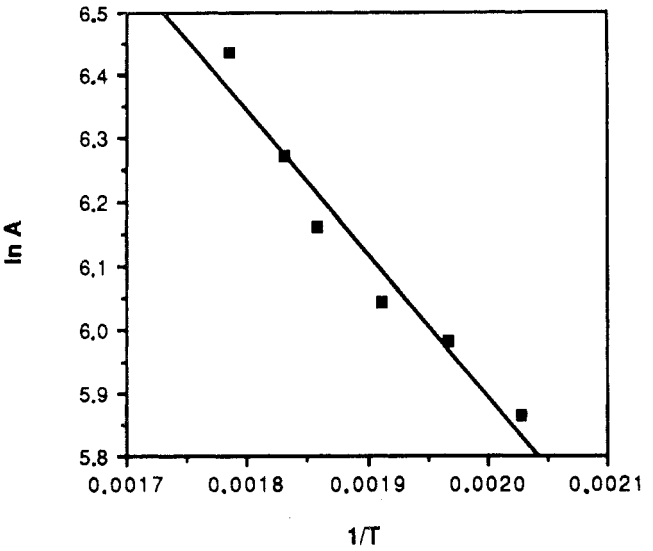

Figure 12. Arrhenius plot of the velocity rate $A(T_c)$.

Similar values had been reported at $T_c = 220$ °C for HBA/HNA copolymers.[1,7]

An Arrhenius plot of the velocity rate $A(T)$ is shown in Figure 12. If the values are linearly extrapolated, an activation energy of $E_a = 18.6$ kJ/mol is calculated, indicating a thermally activated process. Similar values can be found for a HBA/HNA copolymer in the temperature range between 220 and 230 °C.[7] This value is surprisingly low and on the order of the rotational energies for flexible chain molecules.

For rigid aromatic LCP's based on naphthyl and phenyl esters three relaxation processes[15-17] have been reported. An α-process which is associated with the glass transition, a β-process associated with a coordinated rotation of the naphthalene groups around the chain axis, and a γ-process associated with the rotation of the phenyl rings. The latter two relaxation processes exhibit an Arrhenius behavior, with activation energies of 105 (β) and 50 (γ) kJ/mol.[16]

The low value of the activation energy shows clearly that the slow transition process (secondary crystallization process) is not a cooperative process, which would have a much higher activation energy. That may mean that little local motion and local orientation is able to build up crystals or to improve their perfection. Further experiments would be needed to prove this.

(III) Determination of $\Delta H°$ and $T_m°$ at Equilibrium. Determination of the melting temperature $T_m°$ and the heat of fusion $\Delta H°$ for an infinite perfect crystal in equilibrium conditions is always a difficult and controversial matter. Several methods were tried.

On the basis of the experimental data of the heats of transition and transition temperatures, we first extrapolated the melting temperature $T_m°$ and the heat of fusion $\Delta H°$ to infinite crystallization time, according to a procedure proposed by Cheng.[2] Figure 13 shows the extrapolation of the transition temperatures of the highest melting peak against the inverse of log t. This should provide the melting temperature at infinite annealing time $T_m°$ and therefore in the equilibrium state. From the extrapolated curves it can be seen that an exact determination is not possible, but as the rough estimate one can adopt a value of $T_m° = 355 \pm 7$ °C. Figure 14 shows the extrapolation of the reciprocal heat of transition with respect to the reciprocal of log t. Extrapolation provides a heat of transition at equilibrium of about $\Delta H° = 5.7$ kJ/mol.

Determination of the crystallinity by wide-angle X-ray measurements[18] and its relation to ΔH should also give

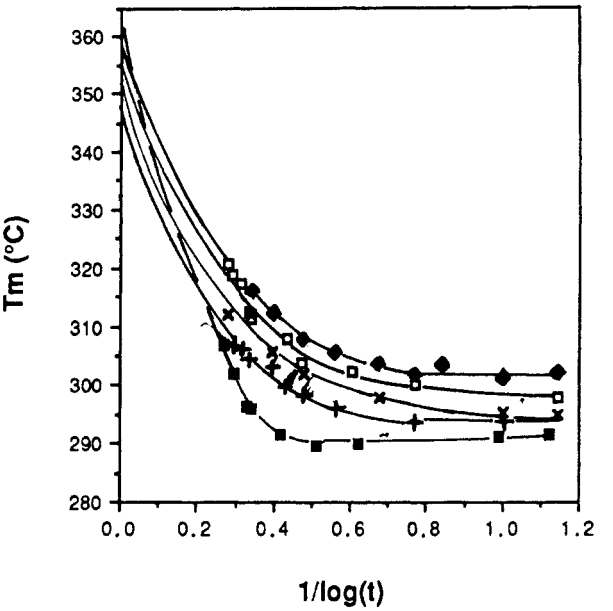

Figure 13. Extrapolation of the temperature of fusion $T_m°$ for infinite crystallization time against the inverse of the logarithm of crystallization time (1/log t) for different temperatures: $T_c = 250$ °C (■); $T_c = 265$ °C (+); $T_c = 273$ °C (×); $T_c = 280$ °C (□); $T_c = 287$ °C (♦).

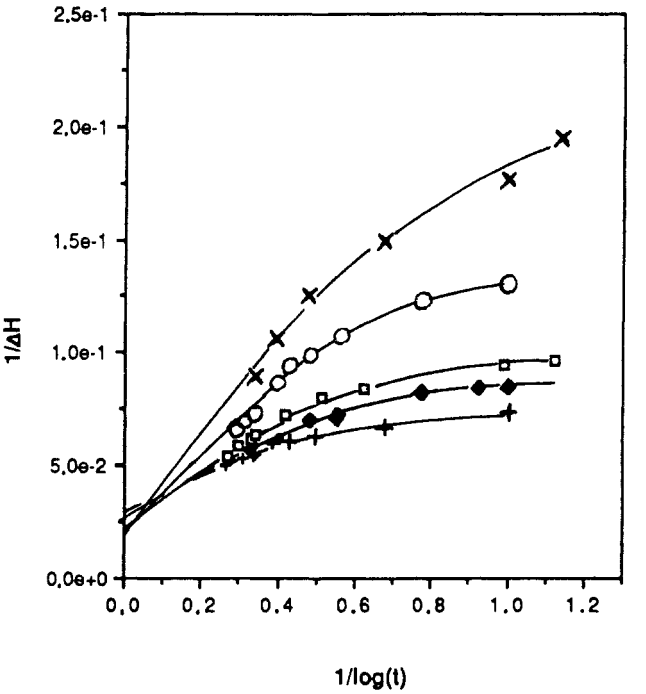

Figure 14. Extrapolation of the reciprocal heat of fusion $1/\Delta H$ for infinite crystallization time against the inverse of the logarithm of crystallization time (1/log t) for different temperatures: $T_c = 220$ °C (+); $T_c = 235$ °C (♦); $T_c = 250$ °C (□); $T_c = 265$ °C (○); $T_c = 273$ °C (×).

the heat of fusion at equilibrium $\Delta H°$. We used a precipitated sample as reference for an "amorphous" sample in order to subtract the amorphous halo from the diffraction peaks of a partially crystalline sample. The word amorphous means that the crystalline size is so small that the line-broadening results in an amorphous halo.[11] The advantage of taking the diffraction pattern of a precipitated sample as a reference compared to the diffraction pattern in the nematic state is that no tentative shifting of the diffraction curve is necessary with respect to the expansion of the structure with temperature. The diffractograms of a precipitated and a long-time crystallized sample are shown in Figure 15. In Figure 16 the crystallinity is plotted versus ΔH for several samples.

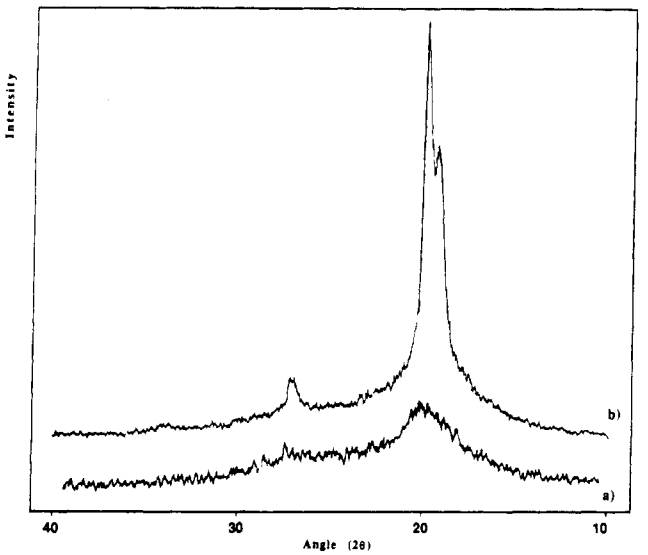

Figure 15. Wide-angle diffractograms for a precipitated sample (a) and a sample which had been annealed for 58 h at 250 °C (b).

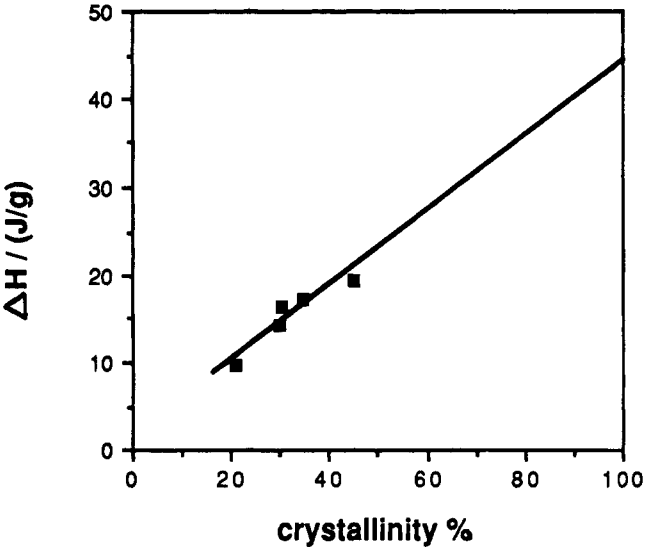

Figure 16. Variation of the crystallinity with the heat of fusion ΔH for different crystallized samples.

Assuming a linear relation between ΔH and crystallinity yields $\Delta H° = 6.3$ kJ/mol for a 100% crystalline sample.

This is in very good agreement with the values determined above. Therefore we keep $\Delta H°$ at 6 kJ/mol (M_w = 143.3). Now it is possible to calculate the transition entropy $\Delta S° = 9.6$ J/(mol K). Similar values are reported in the literature for rigid thermotropic LCP's.[2,7,11,19] We thus have

$$T_m° = 355\ °C;\ \Delta H° = 6\ kJ/mol;\ \Delta S° = 9.6\ J/(mol\ K)$$

These low values of $\Delta H°$ and $\Delta S°$ show clearly the peculiarities of rigid main chain LCP's. The low $\Delta H°$ is directly related to the weak molecular cohesive energy within the crystals, resulting from irregularities (different size of the monomers, bulky side groups, and kinks), whereas the low $\Delta S°$ is directly related to the rigidity of the polymer chain. At the crystalline–nematic phase transition the conformation of the stiff chain does not change very much. The main motion to become apparent may then be a translational motion along the chain axis, since even in the crystalline state there exists a rotational freedom.[15–17,20]

(IV) Isothermal Kinetic Studies. This copolyester has two transition processes. The practical temperature range for an isothermal kinetic study of the fast transition process is limited between 280 and 290 °C. The temperature range for a study of the slow transition process is between 220 and 273 °C.

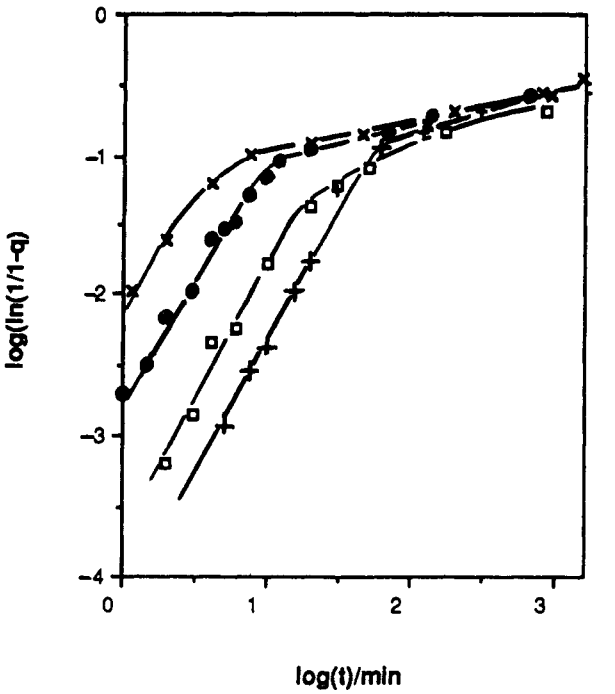

Figure 17. Avrami treatments of the kinetics for the fast transition process at four different crystallization temperatures: T_c = 280 °C (×); T_c = 283 °C (●); T_c = 285 °C (□); T_c = 287 °C (+).

The overall crystallization process can be described by an Avrami equation

$$1 - q = \exp(-kt^n) \qquad (2)$$

where q is the degree of crystallinity given by the ratio of the volume of crystallized material at time t to the total volume, k is the crystallization rate constant, and n is the Avrami exponent containing information about the mode of nucleation and the geometry of the beginning of the growing crystals.[14,21–23]

With the value of $\Delta H°$ determined in the previous section, it is possible to use eq 2. Then $q = \Delta H/\Delta H°$ corresponds to the fraction of crystallinity. An Avrami plot is shown in Figure 17 for crystallization temperatures above 280 °C. It leads to a straight line between log t and log (ln (1/1 − q)). For example one can see that after 10 min at T_c = 283 °C the fast transition process has been nearly completed. The slopes of the straight lines range between 1.98 and 2.05, while at longer crystallization times the slope drops down to n = 0.2.

An Avrami value of n = 2 for other LCP main chain polymers was first reported by Warner and Jaffe[24] and recently reported in refs 3 and 7. When a nucleation controlled growth is adopted with respect to the Avrami equation, this result shows that crystallization of rigid macromolecules can be regarded as an initial two-dimensional growth leading to three-dimensional crystals, if the long axes of the chains are assumed to be parallel in the nematic phase. This assumption is reasonable because in the nematic state order parameters are often larger than 0.8.[1]

In Figure 18, the Avrami treatment for the slow transition process is shown. This transition process is characterized by very low Avrami exponents n, lying in a range between 0.09 at 220 °C and 0.17 at 273 °C. The values of n increase when the crystallization temperature is raised, indicating that the crystal size and crystal perfection are more efficient, the higher the annealing temperature is taken. These low values indicate that this

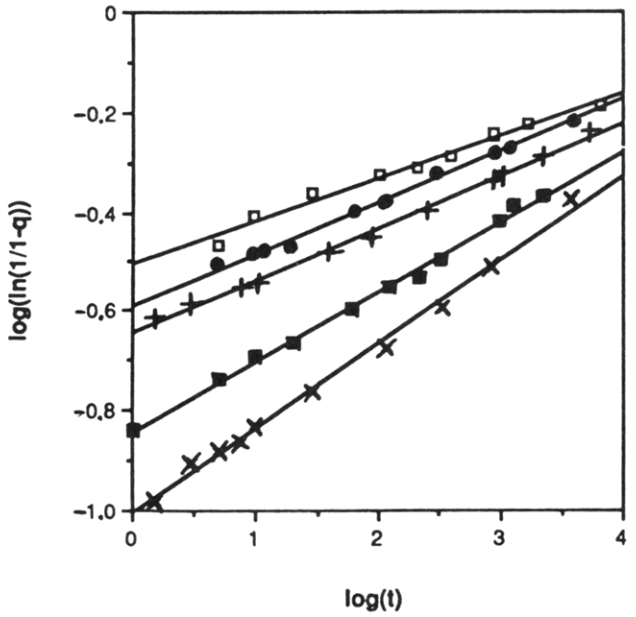

Figure 18. Avrami treatments of the kinetics for the slow transition process at five different crystallization temperatures: T_c = 220 °C (□); T_c = 235 °C (●); T_c = 250 °C (+); T_c = 265 °C (■); T_c = 273 °C (×).

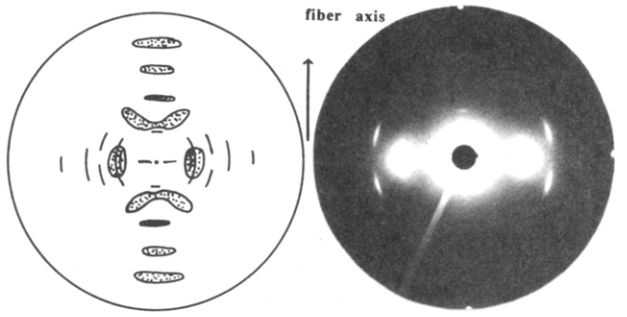

Figure 19. Wide-angle X-ray photograph of a melt-drawn copolyester fiber. The fiber axis lies in the direction of the meridian.

Table I
Calculated and Observed X-ray Reflections

position	2θ/deg exptl	d spacing exptl	d spacing calcd	(hkl)	intensity
eq	18.46	4.74	4.76	(200)	vs
eq	19.30	4.60	4.63	(110)	vs
off eq	26.37	3.38	3.41	(211)	s
eq	33.19	2.70	2.66/2.71	(020)/(310)	m
eq	39.17	2.30	2.31	(220)	vw
m	14.31	6.19	6.3	(002)	s
m	28.42	3.14	3.15	(004)	w
m	37.48	2.40			vw
m	44.41	2.04	2.10	(006)	w

slow process cannot be related to a nucleation and growth process, as for a number of polymers where the same behavior is found. It is more convenient to relate this slow process to a secondary crystallization process.[14]

X-ray Investigations. Determination of the Crystal Unit Cell. Figure 19 shows a diffraction pattern of the investigated copolyester. The fiber axis is in the direction of the meridian. Along the equator, there are four diffraction spots and on the first layer line there is a one off-equatorial reflection. Along the meridian four diffraction spots can be observed. The experimental 2θ angles and the corresponding intensities are listed in Table I. Since the weak meridional reflections cannot be seen on the photo we include a schematic diagram. The number of the X-ray reflections obtained for the crystalline state is surprisingly low despite the fact that the observed reflections are not unusually broad, as can be seen from Figure 15. This indicates that the crystalline state contains a high density of defects.

First the equatorial reflections were indexed to determine the crystal structure. The reflections are in agreement with an orthorhombic structure with a = 9.51 Å and b = 5.31 Å. Since the relation $h + k = 2n$ is fulfilled, the orthorhombic lattice consists of two chains which have their direction along the c-axis.

Adopting the model of Biwas and Blackwell,[10] one should find normally aperiodic meridional scattering for a random copolyester, attributed to variations of the electron density along the chains arising from the random distribution of the comonomers. To describe in their model the off-equatorial reflections, they had to adopt a dimer repeat unit. The copolyester considered here consists of four different structure units. Since a statistical approach would be rather complicated, we used the advantage of having three of the monomers, HBA, TA, and MHQ, which all have the same length of 12.6 Å when associated as dimer repeat units, taking the bond angles and bond lengths from refs 25 and 26. We can thus use the same dimer approach with the fourth one, DDE. We took into account the relative weight of each dimer unit (19.2% for the DDE/HBA and DDE/MQH). This gives a crude approximation for the average c-axis value of c = 13.4 Å, taking into account a length of 16.2 Å for the combinations of DDE with either HBA or MHQ. Taking c-axis values of 13.4 or 12.6 Å gives calculated values of the first layer line reflection (211) which both agree with the observed one.

To find which c-axis value relates better to the crystallographic density ρ_x, we calculated ρ_x and compared it with the density determined by density gradient measurements. This comparison is reasonable, because it was reported that the density of the thermotropic main chain polymers do not change with the degree of crystallinity.[27] Only a c-axis value of 13.4 Å gives an agreement between the calculated and measured densities. In this case, ρ_x is 1.40 g/cm^3 according to

$$\rho_x = (NM_w 1.66)/V \qquad (3)$$

where N = 4 is the number of monomers in the unit cell, M_w = 143.2 denotes the averge molecular weight of a monomer unit, and V = 677 Å^3 is the volume of the average unit cell according to the X-ray determination. The experimental density was measured to be ρ = 1.362 g/cm^3. The good agreement indicates that it is reasonable in our case to calculate an average c-axis length of 13.4 Å only by simple geometric and statistical considerations.

As can be seen from Table I the (00l) reflections are even ordered, indicating that the chain adopts a 2_1 helical conformation along the c-axis, as was found also for the homopolymer of HBA.[28] The reflections fit well, taking a periodic distance of 12.6 Å into account, which is the dimer repeat distance for the HBA, TA, and MHQ combinations. The most obvious discrepancies are only 2.8% for the (006) reflection and 2.5% for the (002) reflection. It has also to be mentioned that the reflection with a d spacing of 2.4 Å could not be indexed. This result indicates that the polymer still possesses a certain periodicity of dimer repeat units which are able to generate such meridional scattering.

The X-ray results give valuable information concerning the DSC experiments. Depending on the cooling rates of nonisothermal crystallized samples, we found different melting peaks for the following heating runs (Figure 2). One of the possible explanations would be that different crystalline structures are present. As can be seen from

the X-ray investigations, there is no observable change in the X-ray diffractograms with respect to cooling rates and crystallization time used in the experiments. That means that only one crystalline structure exists and that the different melting peaks result from crystals with different levels of perfection and sizes.

Conclusions

From the crystallization kinetics for this copolymer and others reported in refs 3, 7, and 24, it seems to be a general feature for rigid rodlike polymers that the crystallization from the nematic melt happens first via thermally activated nucleation in relatively well-ordered domains within the sample. The Avrami exponent for the fast crystallization process always has a value of 2, indicating a two-dimensional growth mechanism, which is in accordance with the behavior of rigid rodlike polymers. Blackwell[10] suggests that the development of a three-dimensional order only requires that one monomer unit on each chain lies about in a register plane perpendicular to the chain axis. If this requirement is fulfilled, only a two-dimensional growth has to happen in a plane perpendicular to the main chain axis. In contrast, the probability of matching different identical sequences of a four-monomer statistical copolymer as it was proposed by Windle and co-workers[9] seems to be extremely small.

The low Avrami exponents for the slow transition process show clearly that it is severely restricted, in spite of its very low activation energy. A possible explanation may be that the observed two-step process of the structure formation is due to a kinetic mechanism that occurs differently at different places within the sample.[1] As mentioned before, crystallization at low cooling rates (see Figure 2) prevents the formation of low-melting crystals. The reason could be that the crystallization process starts in well-ordered domains and becomes severely restricted in the course of the crystallization, at least if part of each chain molecule becomes attached to one growing crystalline region. A reasonable explanation is that any further progress has to occur via translational and reorientational motions of the chains which are fixed to other crystals. This could be the case for crystallization at low cooling rates.

Different melting peaks may then only occur if this fast process is not too quick, giving enough time to build up less perfect crystals. If the cooling rate is increased, the supercooling of the nematic melt is larger and less oriented regions can crystallize. They are stable because lower temperatures are reached before the well-ordered crystals would have physically cross-linked all chains. This effect gets more and more effective with increasing cooling rate.

The slowing down of the Avrami exponents in Figure 14 after a certain crystallinity of about 10%, corresponding to a heat of fusion of 0.6 J/g, can be clearly observed. This results can also be explained by following the proposed model. As mentioned before, we have a two-step process. The rapid crystallization process takes place until the chains are physically cross-linked. The remaining part of the sample and the less perfected crystals can now be transformed into ordered structures only by a slow diffusional process (secondary crystallization). Improvement and growth of the crystal are faster the higher the crystallization temperature chosen.

The activation energy of the slow process has a value of E_a = 18.6 kJ/mol, indicating that the slow process is not cooperative and that the chains possess a high rotational mobility around their long axis. Growth and perfection of the crystals are then due to a slow diffusional motion along the chain axis and to an easy orientational motion around this long axis. An alternative explanation for this noncooperative process could be the movement of defects along the chains. The restricted number of X-ray reflections and the low activation energy for the slow process indicate also that the crystals possess a long-range positional order but that the chains are rotationally disordered along their long axis.

The structure of the crystalline state is difficult to determine exactly because the number of reflections is small and the copolymer is composed of four different monomer units. Nevertheless, we propose an orthorhombic structure with a = 9.51 Å and b = 5.31 Å and with an average c-axis of about 13.4 Å. The density measurements correspond well with the crystallographic density, indicating that the average c-axis length is a reasonable value.

There is nevertheless no clear understanding of the crystalline structure of the copolymer, which seems to be more complex than this simple picture. Two points remain unexplained, the exact c-axis length and the origin of the 2.4-Å reflection.

Acknowledgment. We are grateful to the Rhône-Poulenc Co. for providing the polymer and for financial support. We would like to thank T. De Neve for performing the density measurements. R.L. thanks the Deutsche Forschungsgemeinschaft for a grant.

References and Notes

(1) Butzbach, G. D.; Wendorff, J. H.; Zimmermann, H. J. *Polymer* **1986**, *27*, 1337.
(2) Cheng, S. Z. D. *Macromolecules* **1988**, *21*, 2475.
(3) Cheng, S. Z. D.; Zhang, A.; Johnson, R. L.; Wu, Z.; Wu, H. H. *Macromolecules* **1990**, *23*, 1196.
(4) Wissbrun, K. F.; Griffin, A. C. *J. Polym. Sci., Polym. Phys. Ed.* **1982**, *20*, 1835.
(5) Lin, Y. G.; Winter, H. H. *Macromolecules* **1991**, *24*, 2877.
(6) Lin, Y. G.; Winter, H. H. *Macromolecules* **1988**, *21*, 2439.
(7) Kamal, M. R.; Khennache, O.; Goyal, S. K. *Polym. Eng. Sci.* **1989**, *29*, 1089.
(8) Cheng, S. Z. D.; Janimak, J. J.; Zhang, A.; Zhou, Z. *Macromolecules* **1989**, *22*, 4240.
(9) Hanna, S.; Windle, A. H. *Polymer* **1988**, *29*, 207.
(10) Biwas, A.; Blackwell, J. *Macromolecules* **1988**, *21*, 3146–3158.
(11) Blundell, D. J. *Polymer* **1982**, *23*, 359.
(12) Lenz, R. W.; Jin, J.; Feichtinger, K. A. *Polymer* **1983**, *24*, 327.
(13) Quentin, J. P. Eur. Pat. 191705, 1985.
(14) Wunderlich, B. Vol. II, *Crystal Nucleation, Growth, Annealing*; Macromolecular Physics; Academic Press: New York, 1976; Vol. II.
(15) Blundell, D. J.; Buckingham, K. A. *Polymer* **1985**, *26*, 1623.
(16) Alhaj-Mohammed, M. H.; Davies, M. R.; Abdul Jawad, S.; Ward, I. M. *J. Polym. Sci., Polym. Phys. Ed.* **1988**, *26*, 1751.
(17) Kallika, A. S.; Yoon, D. Y. *Macromolecules* **1991**, *24*, 3404.
(18) Alexander, L. E. *X-Ray Diffraction Methods in Polymer Science*; Wiley & Sons: New York, 1969.
(19) Sauer, T. H.; Zimmermann, H. J.; Wendorff, J. H. *Colloid Polym. Sci.* **1987**, *265*, 210.
(20) Fischer, E. W.; Hellmann, G. P.; Spiess, H. W.; Hört, F. J.; Ecarius, U.; Wehrle, M. *Macromol. Chem. Suppl.* **1985**, *12*, 189.
(21) Avrami, M. *J. Chem. Phys.* **1939**, *7*, 1103.
(22) Avrami, M. *J. Chem. Phys.* **1940**, *8*, 212.
(23) Avrami, M. *J. Chem. Phys.* **1941**, *9*, 117.
(24) Warner, S. B.; Jaffe, M. *J. Cryst. Growth* **1980**, *48*, 184.
(25) Hummel, J. P.; Flory, P. J. *Macromolecules* **1980**, *13*, 479.
(26) Erman, B.; Flory, P. J. *Macromolecules* **1980**, *13*, 484.
(27) Bechtoldt, H.; Wendorff, J. H.; Zimmermann, H. J. *Makromol. Chem.* **1987**, *188*, 651.
(28) Blackwell, J.; Lieser, G.; Guiterrez, G. A. *Macromolecules* **1983**, *16*, 1418.

Registry No. (MHQ)(HBA)(DDE)(TA) (copolymer), 144372-82-7.